The Contribution of Carbon-optimized Battery Electric Vehicle Charging to the Decarbonization of a Multi-modal Energy System

Dominik Husarek, Simon Paulus, Matthias Huber, Michael Metzger, Stefan Niessen
Corporate Technology, Research in Energy and Electronics, Siemens AG
Munich, Germany
dominik.husarek@siemens.com

***Abstract*— Battery Electric Vehicles (BEV) are getting increasing intention when it comes to reaching the emissions targets within the transportation sector. In principle, BEV offer the flexibility to be charged in hours with low CO2 emission. The total amount of such flexibility for the overall energy system is determined in an agent-based simulation and applied within a fully sector-coupling optimization model (electricity, heat, transport). This allows to examine the effects from utilizing this flexibility on reducing the carbon footprint of charging. The flexible share of the BEV charging load is found to be correlated positively with the charging power and reveals that at least 77 % of the charging load can be shifted in time when the charging power peaks. It is shown, that charging processes during working hours can mostly be delayed for 4-9 hours whereas the major share of load while the vehicle is at home has possible delay times of more than 10 hours. While harnessing this flexibility, carbon-optimized charging can further reduce the carbon footprint of BEVs by a maximum 9.1 g CO_2/km which equals 24 % in 2025.**

Keywords—E-mobility, decarbonization, sector coupling, CO_2 intensity, load shifting, agent-based modelling

I. INTRODUCTION

The Intergovernmental Panel for Climate Change recently underlined the importance to restrict global warming to 2 °C as stated within the Paris agreement. To reach this target cross-sectoral (electricity, heat, transport) measures have the potential to contribute greatly to the transformation of the energy system. In this context the road transportation sector is still at its beginning of the transformation showing significant emission reduction potential. Besides other possible technologies, Battery Electric Vehicles (BEV) attract rising interest as key technology. Beyond their primary use for driving, the flexibility potential of BEV can be used to reduce CO_2 emissions in the electricity sector by aligning charging times with the electricity generation from renewable energy sources (RES).

Several works model large-scale aggregated BEV fleets and determine the flexibility potential of the charging process, e.g. Skiba and Moser in [1]. While Schäuble et al. in [2] derive the load shift potential from BEV in terms of exogenously fixed charging strategies, Babrowski et al. in [3] obtain the load shift potential by means of qualitatively determined lower and upper optimization limits. In [4], Zhang et al. published a detailed BEV charging optimization approach with accurate derivation of upper and lower limits for a non-perfect foresight optimization. Their formulation avoids overestimating the possible charging power. Sadeghianpourhamami et al. in [5] use real charging data from BEV and determine the flexibility similar to [4]. With the objective to flatten the charging profile, they conclude that BEV charging at the workplace can be used to fill the afternoon valley and BEV charging at home can be used to fill the night valley.

Seddig et al. in [6] utilize the derived flexibility of BEV charging to integrate RES within a parking garage of 650 BEV showing that the RES utilization can be doubled. The potential reduction of CO_2 emissions from BEV charging is further examined by Howey at al. in [7] and Pasaoglu et al. in [8], where the authors apply annual average CO_2 emissions for the generated electricity. Hourly emissions for electricity are applied by McCarthy and Yang in [9], Hoehne and Chester in [10] and Robinson et al. in [11] whereby they do not consider future scenarios. In contrast, [8] covers the development over several years until 2050. The major distinction of the approach in [9] compared to [10] and [11] is, that the authors do not apply the average emissions over all generating power plants but the hourly emissions of the marginal power plant. Their argument is, that BEV charging increases the load, which has to be satisfied by increasing the generation from the marginally generating power plant. The works of Jochem et al. in [12] as well as Ripp and Steinke in [13] take up on this discussion. In [12], several methods for the determination of emissions related to BEV charging are examined. The authors in [13] published their work regarding the implementation of the calculation of hourly emissions based on the hourly average electricity mix as well as emissions based on the marginal generating power plant. Special emphasis should be given to the fact, that they integrate these methods within the fully sector-coupling energy system development plan model (ESDP) (cf. Müller et al. in [14]).

This paper examines the development of emissions for charging a large fleet of BEV until 2030 in ESDP based on the hourly average emissions for electricity as in [13]. Thereby, charging profiles and the corresponding hourly flexibility of are determined with an agent-based simulation and used as input for the optimization within ESDP. The academic contribution of our work is firstly the hourly quantification of shiftable load and the corresponding maximal delay time for a large fleet of BEV within an agent-based simulation based on real driving data. Secondly, we examine the development of emissions from BEV charging based on endogenously determined CO_2 emissions from electricity within a fully sector-coupling energy system model.

The remainder of the paper is structured as follows. While chapter II focuses on the computation of charging profiles and the corresponding flexibility potential, chapter III derives the hourly carbon footprint of the energy system and shows the resulting implications for emissions of BEV charging with and

without controlled charging. Finally chapter IV discusses the results and chapter V summarizes the work.

II. Modelling of Battery Electric Vehicle Charging

This section focuses on the modelling approach and the assumptions made to derive aggregated BEV charging profiles. On this basis, the main objective of this chapter is to deduce the share of flexible load in dependency of the aggregated charging profiles.

A. Charging profiles

To investigate the impact of BEV on the energy system, aggregated charging profiles of BEV are required. Thus, individual driving profiles of 10,000 BEV based on data of the German mobility study [16] are modelled within an agent-based simulation in NetLogo [17] whereby aggregated charging profiles are computed.

Input

An agent-based model consisting of heterogenous agents each of whom depicting an individually simulated vehicle is applied. The heterogeneity of the fleet is described by the main vehicles' attributes such as battery capacity, the vehicle's consumption and available maximum charging power at the charging station at home or at work. Based on the market shares of electric vehicle models in 2018, the battery capacity varies between 20 kWh and 60 kWh mainly reflecting entry level BEV (e.g. Renault Zoe and Nissan Leaf) and partly premium BEV such as defined in [18] by the International Renewable Energy Agency. For the charging power at home, it is assumed that 90 % of the BEV are using a single phase 16 A charger as provided by the standard 230 V circuit in Germany, which results in a maximal charging power of 3.7 kW. The remaining cars charge with 7.3 kW based on single phase charging with 32 A fuses. By contrast, the charging power at workplaces is uniformly set to 11 kW. It is assumed, that there are no restrictions on the availability of charging stations, which implies that every BEV can connect to the charger whenever it arrives at a charging station at home or at work. Given that the mean electricity consumption of BEV cars is 17.5 kWh per 100 km in 2018 the consumption of each vehicle is normally distributed around this mean value with a standard deviation of 2. On account of this distribution, the consumption rates vary between reasonable values of 13 kWh and 23 kWh per 100 km.

Driving profiles based on real driving data from a German mobility study [16] are used in order to determine the required charging energy of a single vehicle when arriving at a charging station at work or at home. This study is based on a survey comprising 60,713 individuals who recorded their daily driving trips. The allocation of these trips is conducted by randomly assigning daily driving profiles, consisting of several consecutive trips, to each BEV for every simulated day. Thereby the vehicles are clustered into commuters and non-commuters. The group of commuters makes up for 60 % of all trips on working days and 7 % on the weekend [16].

Model

The model for generating hourly charging profiles of BEV can be obtained with the assumption that every BEV starts charging directly at arrival with the maximum available charging power P_n. Hereby, the charging levels of each BEV, at location $n \in \mathcal{N} = \{home, work\}$ are considered, until the BEV departs at t_d or the batteries' state of charge (SOC) reaches 100 % at t_{full}. Fig. 1 illustrates the procedure for an individual BEV for the entire simulation period *T*.

Each BEV has an explicit state which is known for every simulated time step $t \in \mathfrak{T} = \{1, \dots, T\}$. The states "driving" and "parking" are distinguished whereby for the state "parking" different locations are considered. These states are derived from the driving profiles and the corresponding lists T_a and T_d, which consist of all arrival and departure times for the entire simulation period and which are deduced as explained above.

While a BEV is driving, the SOC is reduced according to the BEVs specific consumption and the driven distance $d(t)$ within each hour of the simulated period. The latter is derived from the driving profiles. Every time a BEVs state changes from "parking" to "driving" the next arrival and departure times are selected from the corresponding lists (cf. box "Driving" of Fig. 1).

If a BEVs state is "parking", the charging power is determined and subsequently, the flexibility potential is calculated as described in chapter II B. To determine the charging power, each location *n* differs in its maximal available charging power P_n (cf. TABLE 1). While the battery is not fully charged and not expected to reach a SOC of 100 % in the current time step, the charging power is set to the maximal available charging power at the current BEVs location. If the remaining required charging energy in *t* of a BEV is smaller than the maximal hourly charging energy at the current vehicles' location, the charging power is reduced to the remaining energy required to reach a SOC of 100 % divided by the simulation time interval Δt, which is set to 1 hour. (cf. box "Charge at arrival" of Fig. 1).

Output

Given the individual charging profiles of a BEV $v \in \mathcal{V} = \{v_1, \dots, v_K\}$ with *K* being the number of simulated BEV as in TABLE 1, the aggregated charging profile of all BEV $p_n^{charge,sum}$ at location n is obtained by the summation of all corresponding charging profiles as in (1). Additionally, the total charging profile $p^{charge,sum}$ is obtained by a summation over all locations as in (2).

$$p_n^{charge,sum}(t) = \sum_{v=1}^{K} p_n^{charge}(t), \forall n \in \mathcal{N}, t \in \mathfrak{T} \quad (1)$$

$$p^{charge,sum}(t) = \sum_{n \in \mathcal{N}} P_n^{charge}(t), \forall t \in \mathfrak{T} \quad (2)$$

TABLE 1 PARAMETERS FOR CHARGING PROFILE GENERATION

Parameter	Value	Symbol
Number of simulated BEV within NetLogo	10,000	*K*
Number of considered BEV within ESDP	11.3 mio	-
Charging power home	3.7 kW 7 kW	P_{home}
Charging power work	11 kW	P_{work}
Battery capacity	20, 40, 60 kWh	C_{bat}
Mean consumption	17.5 kWh/100 km	c

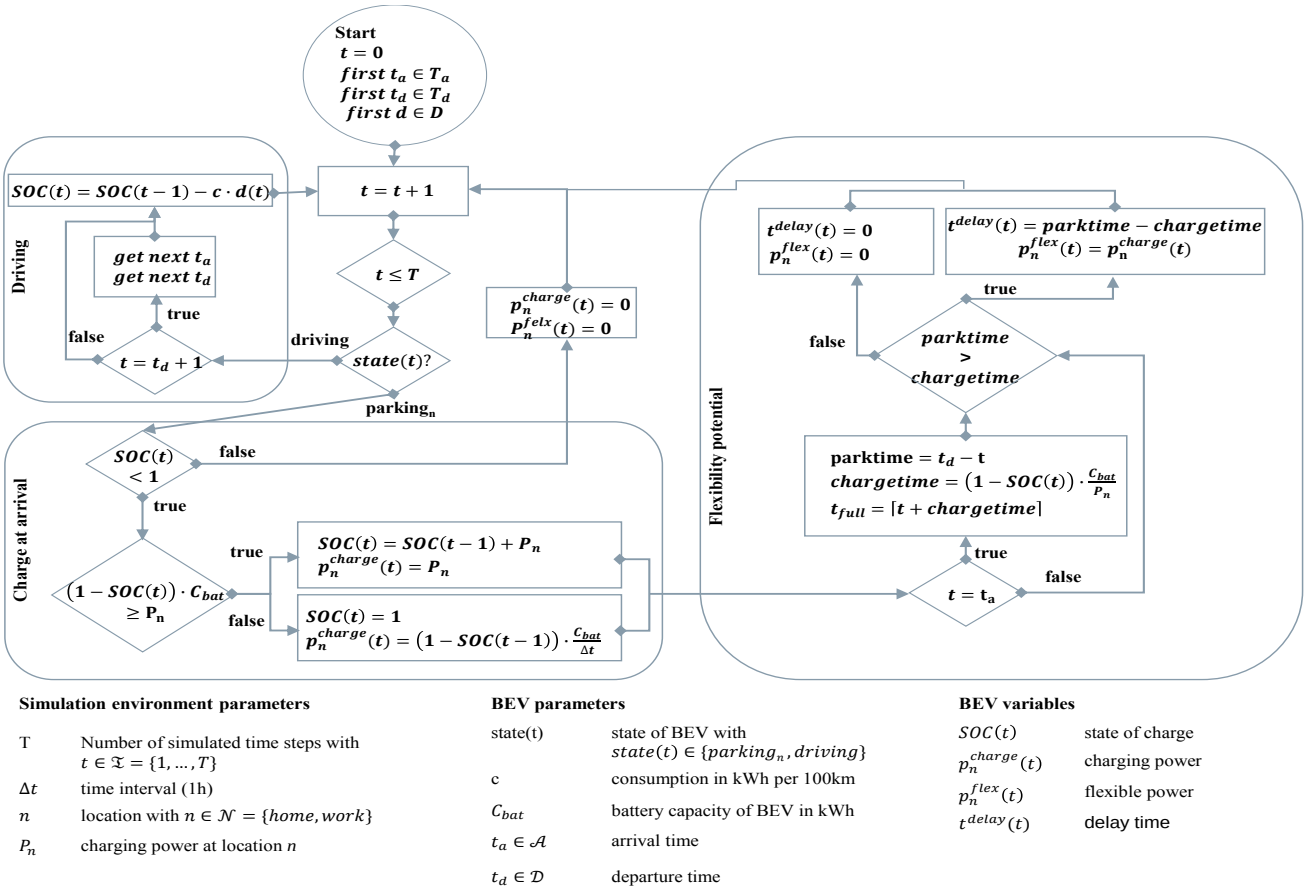

Simulation environment parameters

T	Number of simulated time steps with $t \in \mathfrak{T} = \{1, \dots, T\}$
Δt	time interval (1h)
n	location with $n \in \mathcal{N} = \{home, work\}$
P_n	charging power at location n

BEV parameters

state(t)	state of BEV with $state(t) \in \{parking_n, driving\}$
c	consumption in kWh per 100km
C_{bat}	battery capacity of BEV in kWh
$t_a \in \mathcal{A}$	arrival time
$t_d \in \mathcal{D}$	departure time

BEV variables

$SOC(t)$	state of charge
$p_n^{charge}(t)$	charging power
$p_n^{flex}(t)$	flexible power
$t^{delay}(t)$	delay time

Fig. 1 Flow chart of charging profile generation and determination of flexibility potential for an individual BEV as simulated within agent-based model

Finally, the resulting aggregated charging profiles, which are based on parameters as in table 1 are normed to the total annual charging energy. The profiles vary between days within a week but no seasonal variations are assumed based on minor variations in seasonal driving patterns [16]. The normed profile for an exemplary week is depicted as line "Total charging power" in Fig. 2 and described within the next chapter.

B. Flexibility of Battery Electric Vehicle charging

After determining aggregated charging profiles, this section focuses on the flexibility of the individual and aggregated charging processes. The flexibility f^{sum} of a fleet of BEV is defined by the two parameters $p_{t^{delay}}^{flex,sum}$ and t^{delay}, where $p_{t^{delay}}^{flex,sum}$ is the power at time step *t* which can be delayed for a maximal period of t^{delay}.

Assessing the flexibility potential of a fleet of BEV requires accurate knowledge about the state of each individual BEV. Therefore, at first the flexibility potential f^{ind} of one individual BEV is derived assuming that the vehicle's battery shall be fully charged at the end of the parking period. The procedure is illustrated in Fig. 1.

Model

When a BEV reaches a charging location *n* at $t = t_a$, the duration of the parking session, denoted within the flow chart as "parktime", and the required time to reach a SOC of 100 %, which is denoted as "chargetime", are derived. Furthermore, the time t_{full} when the BEV is fully charged according to the charge at arrival method is computed. The maximal shiftable power and its corresponding delay time t^{delay} are obtained at which the delay time is defined as the difference between the parktime and the chargetime. Note that the delay time is equal for every hour of an entire parking session until the state changes to "driving". For this, we take the simplification that the charging process cannot be interrupted or decelerated by reducing the charging power but only the starting time of the charging process can be shifted in time. This assumption makes the method also applicable to other e.g. industrial processes that may be shifted in time. Further, it is required to quantify the shiftable power p_n^{ind} of a single BEV for the corresponding t_{delay}. Central assumption is that the charging power of a BEV can only be shifted if $p_n^{charge} > 0$ and the duration of the parktime is greater than the chargetime. Moreover, p_n^{flex} can only be reduced by the charging power p_n^{charge} as scheduled when the BEV would immediately charge at arrival (cf. box "Flexibility potential" of Fig. 1).

Output

Consequently, the flexibility f^{ind} of a single BEV can be defined as in (3).

$$f^{ind}(t) = \{p_n^{flex}(t), t^{delay}(t)\}, \forall\, t \in \mathfrak{T} \qquad (3)$$

On this basis, the aggregated flexibility potential in each hour for the entire simulation period *T* of a fleet of BEV can be obtained from the sum of the individual flexibility sets

separately for each value of t^{delay}. Finally, the flexibility for a fleet of BEV can be expressed as in (4).

$$F_v = \left\{ p^{flex}_{t^{delay}}(t), t^{delay}(t) \right\}, \forall\, t \in \mathfrak{T} \qquad (4)$$

Fig. 2 shows the charging power of a fleet of BEV normed to the weekly energy consumption and the corresponding flexibility for each hour of four consecutive days within an exemplary week of the year. The charging profile is separated into home and work charging (cf. (1)) with a peak at 7pm (home) and an additional peak on working days at 9am (work). The figure shows, that the flexible share of the charging power with a mean value of 74 % underlies daily patterns with a daily minimum of 24 % to 29 % (working days) and 37 % to 42 % (weekend) at 5am. Simultaneously, the charging power has a minimum at 5am. The morning peak load on working days, caused by work charging, correlates with a high share of flexibility stating more than 89 % of the load as flexible. While the flexibility during the daily charging peak hour is with 77 % - 78 % (working day) and 81 % - 83 % (weekend) slightly lower compared to the morning peak hours, the daily maximum flexible share of 93 % occurs 3 hours later at 10pm. An in-depth analysis of the correlation between the charging power and the corresponding flexibility potential is visualized in Fig. 3 (a). Looking at the hours in which the charging power at home exceeds the charging power at work, the flexible share has a mean value of 70.4 % and only falls below 52.5 % when the charging power related to the week load is below 0.002 of the week load. This occurs only between 3am and 6am (cf. Fig. 2) when most BEV are already fully charged if they would start charging immediately after arriving. An even higher share of flexibility with a mean value of 86.8 % can be seen for hours in which the work charging power exceeds the home charging power. During these hours the flexibility never falls below 59.2 %.

Moreover, the flexibility potential represented in Fig. 2 is differentiated by delay times whereas the delay times are summarized in intervals for better visualization. The graph shows that the load, which can be shifted for more than 12 hours, increases during the day until 7pm and decreases to zero until 1am. The night hours after 8pm are dominated by load, which can be shifted for 7 to 12 hours whereas the flexible load with higher delay times reduces as time progresses until the morning hours. During work charging dominated hours between 7am and 11am, the major share of flexible load can be shifted for 4-9 hours. These delay times are subsequently defined as medium term flexibility. The share of short term flexibility in contrast, with a maximal delay smaller than 4 hours, rises from 7am until 10am. The consecutive hours until 3pm are dominated by short term flexibility. Fig. 3 (b) summarizes the share of load which can be shifted for a specific delay time and distinguishes between home charging and work charging dominated hours. Main finding from this graph is, that home charging dominated hours which were found to have a lower mean value of flexible load occur to have longer possible delay times with 57 % of the flexible load being able to shift for at least 12 hours. By contrast, 73.8 % of the flexibility of work charging dominated hours occurs to be medium term flexibility. This difference can be traced back to the parking time at work which is typically shorter than the parking time at home.

III. Carbon Footprint Calculation of BEV Charging

In order to determine the carbon footprint of BEV charging as in chapter III C, an hourly CO_2 intensity is calculated in chapter III B based on a multi-modal energy system model as described in chapter III A.

A. Energy System Development Plan

The multi-modal energy system development plan (ESDP) is a mixed-integer linear optimization tool with the objective to determine a cost-optimal decarbonization pathway over several years as well as the optimal dispatch of all technologies for each hour of the year. Additionally, it is a fully sector-coupling model considering electricity, heat, cooling and transportation.
The main constraint driving the transition of the system is the CO_2 limit, which can either be implemented as a price, reflecting a CO_2 tax, or as a total amount, where the CO_2 price is determined endogenously based on the binding CO_2 limit [14].

Within this paper, a multi-modal transformation pathway from 2015 to 2030 for the German energy system is derived based on a socio-, techno-economic scenario that has been

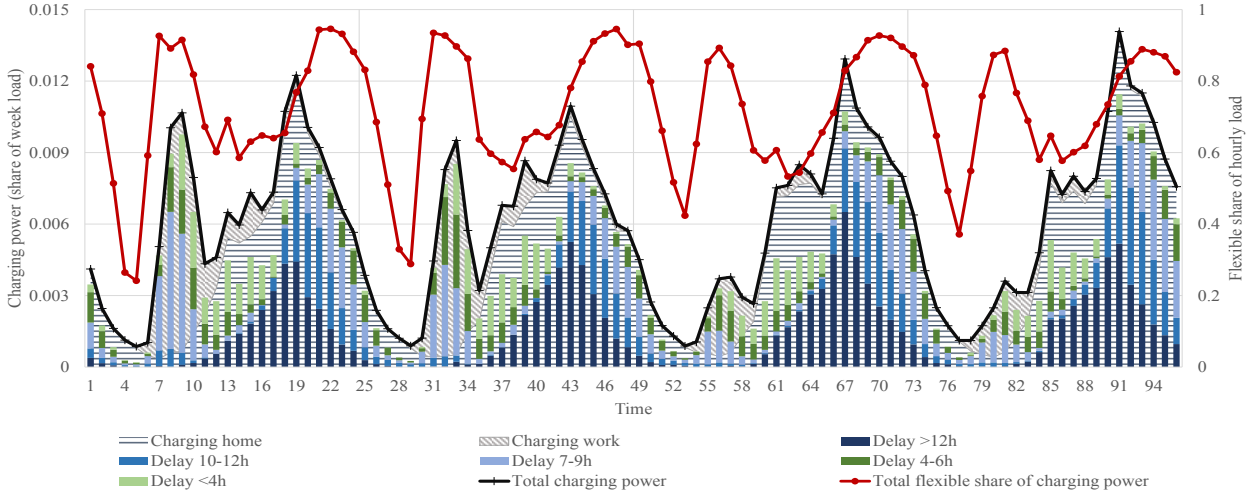

Fig. 2 Normed charging power at home and work as well as corresponding flexibility potential differentiated by delay times in each hour of four consecutive days within an exemplary week

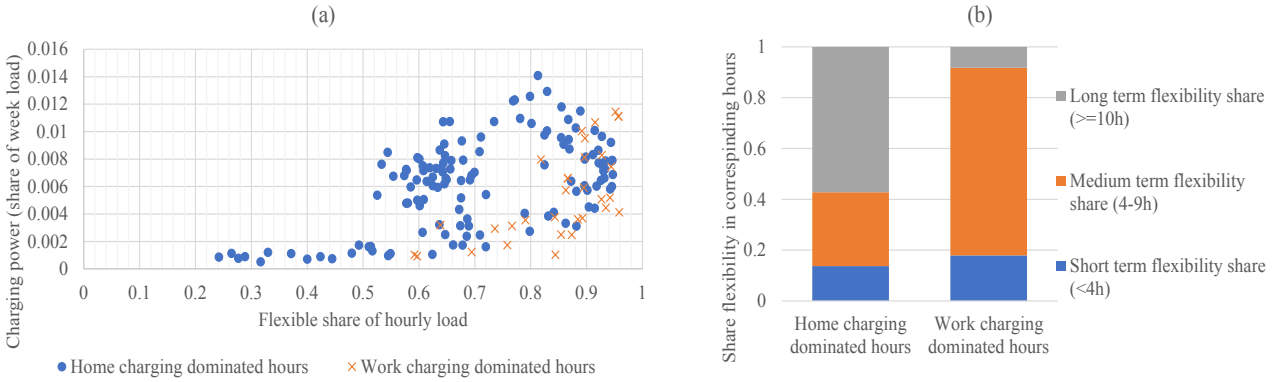

Fig. 3 (a) Correlation between charging power and flexibility potential and (b) delay time of load during work and home dominated hours

developed with partners of the German publicly funded Kopernikus research project ENSURE. The scenario is shaped by the ambitious CO_2 reduction objective of 78 % across all sectors until 2030. This requires severe measures such as a strong electrification of heat and traffic. Additionally, a decline in exogenous electricity demand is assumed within the scenario. Hence, an annual electricity consumption by BEV in 2030 of 29 TWh is assumed within the scenario being equivalent to about 11.3 mio cars. For computational reasons only four representative weeks within each modelled year are computed.

The derived charging profiles as described in chapter II are used within ESDP as input. Therefore, the profile is scaled to an annual electricity consumption of 29 TWh. To validate the upscaling, the number of simulated cars has been varied within the agent-based simulation showing, that the normed load profiles do not differ significantly when the number of BEV is increased above 10,000. The optimization of these profiles is based on a load shifting approach according to Zerrahn and Schill [19] enabling the detailed integration of the derived flexibility of BEV charging as described in chapter II.B. As explained before, we assume that a specified share of charging power can be shifted for a specified delay time. Thereby, it is ensured that the total energy stays constant and load is only shifted in time but not curtailed. This general approach was modified for the specific use case of BEV charging as follows. First, load can only be shifted into the future, since the BEV charging profiles are based on the assumption, that cars are able to start charging immediately after their arrival. Secondly, the newly generated profile is limited to the maximum peak load of the original load profile. This ensures that load shifting of BEV charging cannot increase the peak power and thus grid overloading is avoided. This means that we assume, that all grid constraints even within low voltage grids are not exceeded by the original profile. Finally, the consideration of accurately determined delay times ensures that the charging power of a BEV is still available from the same BEV at the same location when the load is shifted within this delay time period.

B. Determining the hourly carbon footprint of electricity

In order to accurately determine the emissions that accrue during the charging process of a fleet of BEV, knowledge of the so called As-Is CO_2 Intensity I^{As-Is} of the commodity electricity is required [13]. The idea is to assign emissions, which emerge within the multi-modal energy system, to all kinds of commodities equally by adding up all CO_2 emissions related to the generation of electricity and dividing by the total amount of produced energy in the considered hour. The main difference to other approaches, such as published by Stoll et al. in [20], is that they mostly assign the emissions only to electricity and, for instance, do not consider sector coupling and large-scale storage. The mathematical calculation within a multi-modal energy system as implemented in ESDP is extensively described in [13]. On this basis, henceforth we only cover the description of the basic assumptions considered within the modelling process:

- CO_2 emissions are distributed among all considered commodities based on their corresponding energy outflows. Considered energy outflows are all energy outflows, which are useful energies and are not considered as losses.
- Only emissions, which accrue within the system boundaries by converting primary energies into secondary energies are accounted for. Imported secondary energies such as electricity from beyond the system borders are considered as carbon neutral.
- Exporting electricity or heat from the system does not reduce the total emissions within the system boundaries.
- Only operational emissions from primary fuel conversion are considered. Life cycle emissions for the technology and infrastructure are neglected.

Fig. 4 shows the hourly electricity generation per technology as well as the corresponding CO_2 intensity for an exemplary summer week in 2025 for the scenario SLB as described in the previous section. It is apparent, that daily CO_2 intensity patterns emerge that can be traced back in particularly to the volatile electricity generation from renewable energy sources (RES). The CO_2 intensity varies between 0 t/MWh and 0.64 t/MWh. It can be seen, that the PV dominated electricity generation between 8am and 5pm with up to 60 GW supply from PV displaces all conventional technologies during these hours, which subsequently reduces the CO_2 intensity to zero. Lignite and coal power plants add up to 15 GW predominantly in hours with low PV and wind feed-in during the night. Thereby, two different CO_2 intensity levels can be identified during the night. Firstly, the nightly CO_2 intensity peak, which occurs at about 2am, varies from

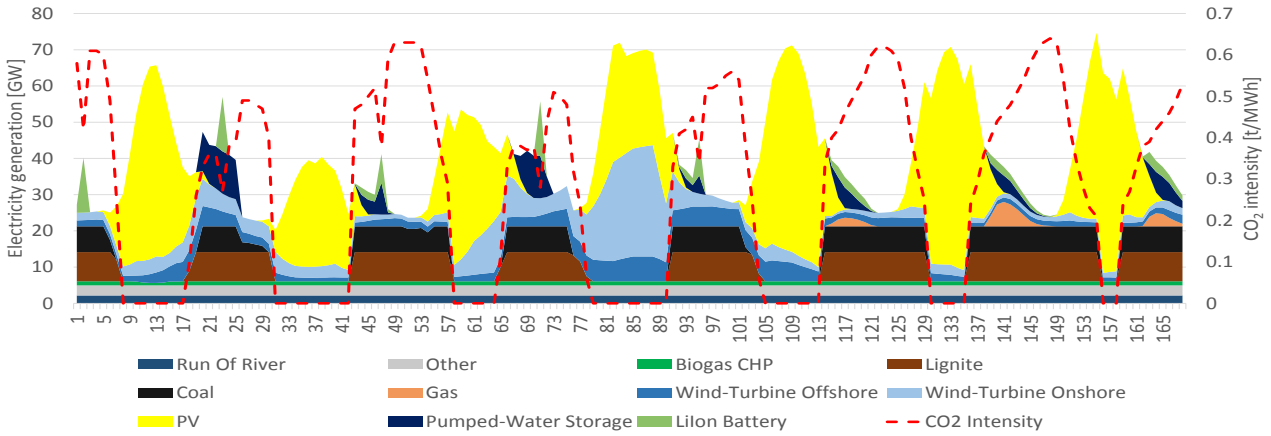

Fig. 4 Hourly electricity generation (left ordinate) and CO_2 intensity (right ordinate) for an exemplary summer week in 2025. Imported electricity is not depicted within this diagram since it is considered as carbon-neutral.

day to day between 0.5 t/MWh and 0.64 t/MWh. Secondly, at about 10pm the intensity varies between 0.36 t/MWh and 0.45 t/MWh. The difference between 10pm and 2am is mainly caused by the utilization of pumped-water storage and Li-Ion batteries. These storage technologies are charged when electricity is cheap at hours with high electricity generation from RES which correlates with low CO_2 intensities as described in [20] and verified for the modelled scenario SLB. Since the CO_2 intensity while charging these storages is considered, the outflowing low carbon related electricity from storage reduces the CO_2 intensity of electricity within the corresponding hours.

In addition, it holds that CO_2 emissions from heat and electricity generating technologies (lignite, coal and gas power plants) are prorated to both commodities by their hourly energy output, which basically reduces the emissions assigned to electricity. After all, the differences between the nightly CO_2 intensity peaks primarily emerges from differences in the total hourly generated electricity and the produced heat from lignite, coal and gas power plants.

The transition of the energy system between 2015 and 2030 is driven by the ambitious decarbonization targets. By that, the generation technologies, as depicted in Fig. 5 (a), change rapidly. The graph reveals, that after the nuclear phase out in 2022 also lignite and coal power plants phase out completely until 2030. It is apparent, that the omitted conventional electricity generation is replaced by RES representing about 58 % and 73 % of the total electricity generation in 2025 and 2030 respectively. The predominant renewable technologies in 2030 are onshore wind-turbines, which account for 188 TWh respectively 38 % of the total electricity production. They are accompanied by 64 TWh from offshore wind-turbines and 73 TWh from PV, whose major share is generated during the summer months. These highly volatile generation technologies are complemented by 94 TWh from gas turbines, which are less carbon-intensive than coal power-plants and more flexible. Nevertheless, it is necessary to harness the volatile electricity production by means of flexible demand, which mainly comes from power-to-heat technologies such as resistive heaters with large thermal storages. Optimized BEV charging can add to this flexibility and this effect is investigated here.

Fig. 5 (b) compares the annual CO_2 intensity distributions, which result from the previously described generation mix, from 2015 to 2030 using box plots for easy quantification and comparison. This depiction is revealing in several ways. First, the mean value from 2015 to 2025 decreases almost linearly from 0.42 t/MWh to 0.22 t/MWh before it drops down to 0.05 t/MWh in 2030 due to the coal phase out. Additionally, the reduction of the mean value from 2020 to 2025 is slightly less than in the first 5 years due to the displacement of all remaining nuclear power plants. Second, the upper whisker showing the hours with the maximum CO_2 intensity stays almost constant until 2025 between 0.64 and 0.66 t/MWh. These high values occur during coal dominated hours. A

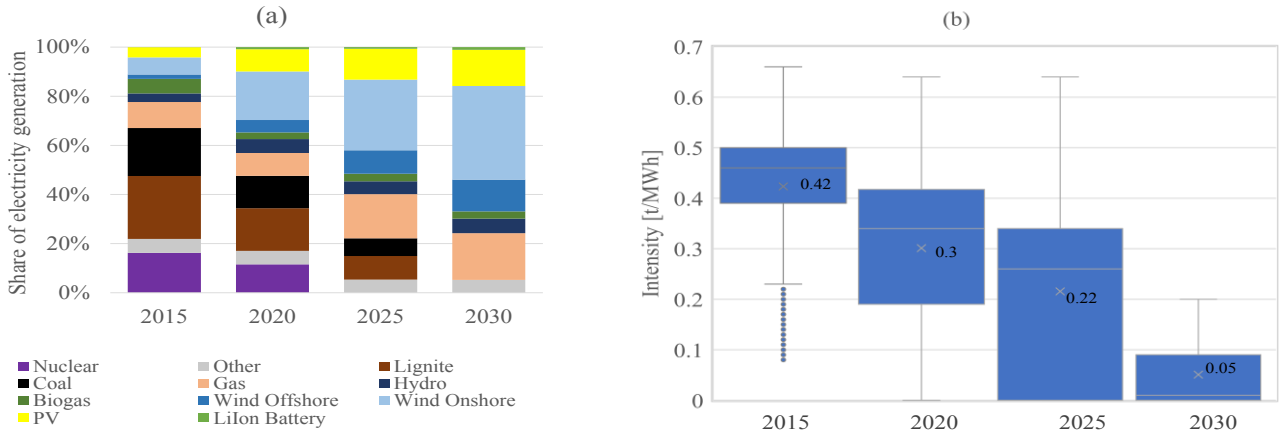

Fig. 5 (a) Annual electricity generation and (b) annual CO2 intensity distribution

significant drop in 2030 down to 0.2 t/MWh is an indication for a coal-free system, where the CO_2 intensive hours are dominated by heat and electricity producing gas power plants. Third, the inter-quartile range, which is depicted as filled box and which represents the middle 50 % of all hours in terms of CO_2 intensity, increases until 2025 and significantly decreases in 2030. This allows for quantified statements about the volatility of the CO_2 intensities and it is indicative for the potential of optimized charging since load can theoretically be shifted from CO_2 intense hours to hours with a very low or even zero CO_2 intensity. The graph reveals that the highest volatility and thereby the highest potential for carbon optimized charging is in the year 2025 with the upper whisker at 0.64 t/MWh, the lower quartile at 0 t/MWh indicating a high share of carbon-neutral hours and the upper quartile being at 0.34 t/MWh. Based on this, the subsequent analysis regarding the carbon footprint of BEV charging and the potential benefits from optimized charging, focuses on the year 2025.

C. *Carbon footprint of BEV*

Finally, the hourly emissions assigned to the charging of a fleet of BEV is calculated based on the hourly CO_2 intensity and the aggregated charging profile, which depends on the annual BEV penetration. *Fig.* 6 (a) shows the resulting total annual emissions from BEV charging each year. The depicted penetration level of BEV is based on the total amount of 44.4 mio passenger cars in Germany [21]. It can be seen, that the occurring amount of CO_2 caused by uncontrolled charging is 3 mio tons in 2020, when 9.7 TWh are generated to satisfy the mobility demand of 3.8 mio BEV. In 2025 the amount of BEV doubles to 7.5 mio BEV, which corresponds to a BEV penetration of 17 %. The CO_2 emissions in contrast only increase by 40 % to 4.22 mio tons. This comparatively low increase is due to the simultaneously increasing share of RES and hence the decreasing mean CO_2 intensity as described above. It is noticeable that from 2025 to 2030 the total CO_2 emissions drop significantly down to 1.62 mio tons, despite the further increase of BEV within the system to a penetration level of 25 % (11.3 mio cars). This is due to the coal phase out and the further rising penetration level of RES reaching 72.2 % in 2030.

Besides major investments in RES and hence a reduced CO_2 intensity for electricity, the controlled charging of BEV within its flexibility limits can reduce the total emissions from passenger cars. The main impact can be seen in 2025 where 7.5 mio BEV with controlled charging produce only 7.7 % more tons of CO_2 than 3.8 mio BEV with uncontrolled charging in 2020. This amounts to a CO_2 reduction from controlled charging of 1 mio tons of CO_2 in 2025.

Fig. 6 (b) shows additionally the specific emissions per driven kilometre for BEV. The specific emissions with uncontrolled charging decrease from 75.1 g CO_2/km in 2015 to 9.8 g CO_2/km in 2030. The impact of carbon optimized charging is strongest in 2025 as described above. The reduction potential in 2025 amounts to 9.1 g CO_2/km, which is about 24 % of the specific emissions.

IV. Discussion

The aim of this paper is to determine the potential benefit of carbon optimized BEV charging for the decarbonization of the energy system. Our assessment of the flexibility potential shows that the aggregated charging profile consists of a significant amount of flexibility, which can be used if it is incentivized. It reaches a maximum of 6.34 GW at 7 pm on the weekend. In addition, charging at workplaces should be incentivized by politics in order to harness the flexibility supporting PV integration into the grid. The measured impact of carbon optimized charging on the emission reaches its maximum in 2025. Whether or not this result can be transferrable to other countries with an electricity mix dominated by RES where CO_2 intensive power plants are still operating has to be further analyzed. The applied method for the computation of hourly CO_2 intensities, was chosen instead of a method based on the marginal generating power plant as in [9] in order to be able to assess also a substantial share of BEV. Not shown in this paper but investigated is the impact of substituting internal combustion cars with BEV. It was found that, the operational emissions can be reduced and reach out far more than the optimized charging. In terms of abatement costs, the controlled charging is significantly less cost-intensive and can serve as argument to promote BEV for customers with a green attitude.

Even if the carbon reduction potential within a system without carbon intensive power plants and about 70 % of RES as in the chosen scenario within this paper is in absolute terms low, the determined flexibility potential of BEV can contribute in terms of grid serving flexibility in order to

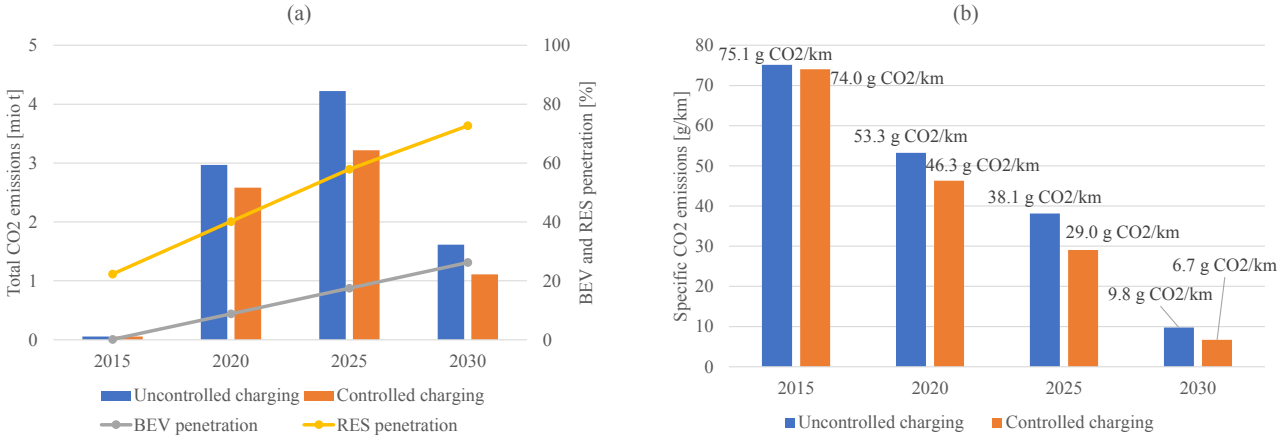

Fig. 6 BEV charging emissions from 2015 to 2030 with uncontrolled and controlled charging

alleviate congestions. Additionally, the need for short term flexibility in terms of ancillary services such as frequency and voltage control to support system stability can be supported by controlled BEV charging in the future [22].

V. Conclusion and Outlook

This paper shows that the flexibility of BEV charging, which is derived based on real driving data, is above 77 % during peak hours for charging at home with possible delay times of more than 10 hours. The flexible share during work peak load hours exceeds 89 % with delay times of 4-9 hours. Therefore, it is found that incentivizing flexible charging at work would greatly contribute to reduce the CO_2 emissions. Finally, we conclude that flexible charging has the potential to reduce 1 mio tons of CO_2 accounting to a decline of specific emissions of 9.1 g CO_2/km or 24 % respectively.

Further work has to be done in analysing impact factors on the flexibility potential such as public charging and limited availability at charging stations. Additionally, an extension of the work aiming at integrating large depots with electric busses or delivery vehicles is interesting. Moreover, capabilities to exploit the theoretically determined maximal flexibility potential should be analysed. Thereto, possible incentives like different tariff structures on the individual BEV level or the implementation of local energy markets may be subject to further research.

Acknowledgement

This work was conducted in the course of the research project ENSURE (FKZ 03SFK1F0) and supported by the German Federal Ministry of Education and Research (BMBF).

References

[1] L. Skiba and A. Moser, “Modeling Large Electric Vehicle Fleets in Power System Simulations,” in *2018 15th International Conference on the European Energy Market (EEM)*, Lodz, 2018, pp. 1–5.

[2] J. Schäuble, T. Kaschub, A. Ensslen, P. Jochem, and W. Fichtner, “Generating electric vehicle load profiles from empirical data of three EV fleets in Southwest Germany,” *Journal of Cleaner Production*, vol. 150, pp. 253–266, May 2017.

[3] S. Babrowski, H. Heinrichs, P. Jochem, and W. Fichtner, “Load shift potential of electric vehicles in Europe,” *Journal of Power Sources*, vol. 255, pp. 283–293, Jun. 2014.

[4] H. Zhang, Z. Hu, Z. Xu, and Y. Song, “Evaluation of Achievable Vehicle-to-Grid Capacity Using Aggregate PEV Model,” *IEEE Transactions on Power Systems*, vol. 32, no. 1, pp. 784–794, Jan. 2017.

[5] N. Sadeghianpourhamami, N. Refa, M. Strobbe, and C. Develder, “Quantitive analysis of electric vehicle flexibility: A data-driven approach,” *International Journal of Electrical Power & Energy Systems*, vol. 95, pp. 451–462, Feb. 2018.

[6] K. Seddig, P. Jochem, and W. Fichtner, “Integrating renewable energy sources by electric vehicle fleets under uncertainty,” *Energy*, vol. 141, pp. 2145–2153, Dec. 2017.

[7] D. A. Howey, R. F. Martinez-Botas, B. Cussons, and L. Lytton, “Comparative measurements of the energy consumption of 51 electric, hybrid and internal combustion engine vehicles,” *Transportation Research Part D: Transport and Environment*, vol. 16, no. 6, pp. 459–464, Aug. 2011.

[8] G. Pasaoglu, M. Honselaar, and C. Thiel, “Potential vehicle fleet CO2 reductions and cost implications for various vehicle technology deployment scenarios in Europe,” *Energy Policy*, vol. 40, pp. 404–421, Jan. 2012.

[9] R. McCarthy and C. Yang, “Determining marginal electricity for near-term plug-in and fuel cell vehicle demands in California: Impacts on vehicle greenhouse gas emissions,” *Journal of Power Sources*, vol. 195, no. 7, pp. 2099–2109, Apr. 2010.

[10] C. G. Hoehne and M. V. Chester, “Optimizing plug-in electric vehicle and vehicle-to-grid charge scheduling to minimize carbon emissions,” *Energy*, vol. 115, pp. 646–657, Nov. 2016.

[11] A. P. Robinson, P. T. Blythe, M. C. Bell, Y. Hübner, and G. A. Hill, “Analysis of electric vehicle driver recharging demand profiles and subsequent impacts on the carbon content of electric vehicle trips,” *Energy Policy*, vol. 61, pp. 337–348, Oct. 2013.

[12] P. Jochem, S. Babrowski, and W. Fichtner, “Assessing CO2 emissions of electric vehicles in Germany in 2030,” *Transportation Research Part A: Policy and Practice*, vol. 78, pp. 68–83, Aug. 2015.

[13] C. Ripp and F. Steinke, “Modeling Time-dependent CO2 Intensities in Multi-modal Energy Systems with Storage,” *arXiv:1806.04003 [eess]*, Jun. 2018.

[14] C. Müller *et al.*, “Modeling framework for planning and operation of multi-modal energy systems in the case of Germany,” *Applied Energy*, vol. 250, pp. 1132–1146, Sep. 2019.

[15] P.-H. Li and S. Pye, “Assessing the benefits of demand-side flexibility in residential and transport sectors from an integrated energy systems perspective,” *Applied Energy*, vol. 228, pp. 965–979, Oct. 2018.

[16] R. Follmer *et al.*, “Mobilität in Deutschland 2008: Ergebnisbericht: Struktur - Aufkommen - Emissionen - Trends",” Bonn, Berlin, 2010.

[17] U. Wilensky, *NetLogo, http://ccl.northwestern.edu/netlogo/*. Center for Connected Learning and Computer-Based Modeling, Northwestern University, Evanston, IL, 1999.

[1] International Renewable Energy Agency, “Innovation outlook: Smart charging for electric vehicles,” p.27, Abu Dhabi, 2019.

[19] A. Zerrahn and W.-P. Schill, “On the representation of demand-side management in power system models,” *Energy*, vol. 84, pp. 840–845, May 2015.

[20] P. Stoll, N. Brandt, and L. Nordström, “Including dynamic CO2 intensity with demand response,” *Energy Policy*, vol. 65, pp. 490–500, Feb. 2014.

[21] Kraftfahrt-Bundesamt, “Bestandsbarometer Personenkraftwagen am 1. Januar 2015 nach ausgewählten Merkmalen.” .

[22] VDE|FNN, “Metastudie Forschungsüberblick Netzintegration Elektromobilität,” FGH e.V., Dec. 2018.